

Electronic Supplementary Information (ESI)

Novel specific peptides as superior surface stabilizers for silver nano structures: Role of peptide chain length

Manuel Ahumada,^{a†} Erik Jacques,^{a†} Cristina Andronic,^a Jeffrey Comer,^b Horacio Poblete,^{c*}
and Emilio I. Alarcon^{a,d*}

^aDivision of Cardiac Surgery Research, University of Ottawa Heart Institute, 40 Ruskin Street, Ottawa, Canada. ^bInstitute of Computational Comparative Medicine, Nanotechnology Innovation Center of Kansas State, and Department of Anatomy and Physiology, Kansas State University, Kansas, USA. ^cCenter for Bioinformatics and Molecular Simulations, Facultad de Ingeniería, Universidad de Talca. ^dDepartment of Biochemistry, Microbiology, and Immunology, Faculty of Medicine, University of Ottawa, Ottawa, Canada. † Authors contributed equally to this work.

*Corresponding author

E-mail: ealarcon@ottawaheart.ca; hoboblete@utalca.cl

Page S1. This page

Page S2. Materials and Methods

Page S8. Figure S1

Page S9. Figure S2

Page S10. Figure S3

Page S11. Figure S4

Page S12. Figure S5

Page S13. Figure S6

Page S14. Figure S7

Page S15. Figure S8

Page S16. Figure S9

Page S17. References

Materials and Methods

Chemical reagents

Silver nitrate (AgNO_3), 2-Hydroxy-1-[4-(2-hydroxyethoxy)phenyl]-2-methyl-1-propanone (I-2959), *N*-(3-Dimethylaminopropyl)-*N'*-ethylcarbodiimide hydrochloride (EDC), *N*-Hydroxysuccinimide (NHS), Trisodium 2-hydroxypropane-1,2,3-tricarboxylate (sodium citrate), 2-morpholinoethane sulfonic acid monohydrate (MES), sodium hydroxide (NaOH), chondroitin sulphate, phosphate buffered saline (PBS) and sodium chloride (NaCl) from Sigma-Aldrich were used as received. Custom synthesized peptides: P1: (CLKGP – Hyp – NH_2 , M-H+ = 629.59), P2: (CLKGP – Hyp – GP – Hyp – GP – Hyp – NH_2 , M-H+ = 1164.28) and P3: (CLKGP – (Hyp – GP)₄ – Hyp – NH_2 , M-K-H-2+ = 879.90) from (purity > 95%) abm[®] and Type I porcine collagen Theracol (1%) from Sewon cel contech were used as received. Unless otherwise indicated all solutions were prepared using Milli-Q water.

Synthesis of citrate capped AgNPs

Citrate capped AgNPs (AgNP@citrate) were prepared according to a previously described protocol.¹ Briefly, an aqueous solution containing 0.2 mM AgNO_3 , 0.2 mM I-2959 and 1mM of citrate (or sodium citrate) was prepared and purged with N_2 for 30 min to deoxygenate the solution. Once purged, the solution was irradiated with UVA light (8 lamps) at 25 °C in a temperature controlled Luzchem LZC-4 photoreactor for 30 min. Yellow translucent solutions were obtained in all cases and were kept at room temperature protected from light.

Replacement of the capping agent with CLK-like peptides

Freshly made AgNP@citrate solutions were split in same volume aliquots and injected with one of the following peptides: P1 (CLKGP – Hyp – NH_2), P2 (CLKGP – Hyp – GP – Hyp – GP – Hyp – NH_2) and P3 (CLKGP – (Hyp – GP)₄ – Hyp – NH_2). The peptide concentrations used to test the capping agent replacement for each peptide were 5, 20, 50, 80 and 100 μM .

Synthesis of AgNPs capped with peptides

AgNPs directly capped with the peptides were prepared following the same protocol described above for AgNP@citrate with minor modifications. Briefly, the citrate was replaced with one of the peptides (P1, P2, or P3) and three different final concentrations of peptides were prepared (0.5, 1 and 5 μM). N_2 purging time was 45 min and irradiation time was 60 min. The evolution of the reaction was monitored at the surface plasmon band (SPB) using spectral scanning with a Libra S50 UV-Vis spectrophotometer (Biochrom, Cambridge, UK) at the following times: 0, 1, 3, 5, 10, 15, 20, 30 and 60 min. For both types of AgNPs, some samples were kept in a colloidal suspension for characterization and the rest freeze-dried for 4 days with a Freezone 6 L freeze-dryer (Labconco®, Kansas City, USA).

Transmission electron microscopy (TEM)

Briefly, 5 μL of fresh samples of AgNP@peptide (P1, P2 or P3) with final peptide concentrations of 0.5, 1 and 5 μM were put onto carbon-coated copper grids (400 mesh) and dried in a vacuum system for 3 days. Electron microscopy images were obtained in a JSM-7500F FESEM from JEOL Inc., working in the transmission mode (TEM) at 15 kV. Additional, high resolution TEM for elucidating crystalline lattice of the samples containing 1.0 μM of P2 and P3 were carried out in a FEI Tecnai G2 F20 TEM system operating at 200 kV.

Hydrodynamic sizes and zeta potential measurements

Changes in hydrodynamic sizes by dynamic light scattering (DLS) and zeta potential (ζ) measurements to quantify the stability of AgNP@peptides solutions were carried out in a Zetasizer Nano ZS (Malvern Instruments Ltd., Malvern, UK) using disposable folded capillary cells at 25°C. Reported values correspond to the an average of three independent batches, each measured in triplicated.

Stability assessments

To get information regarding the ionic stability of the NPs, ionic stress tests were performed by following the changes in the SPB of nanoparticles immersed in a saline solution. For AgNPs under capping agent replacement a 0.9% NaCl solution was tested, with P1, P2 or P3 at 20 μ M and 100 μ M final concentrations. AgNPs directly capped with the peptides (at 5 μ M final concentration), were tested using a 1.8% NaCl solution. The SPB was followed by spectral scanning using a Synergy Mx multi-mode microplate reader (BioTEK, Winooski, USA).

Additionally, AgNPs with the replaced capping agent (P1, P2 and P3) were subjected to further stability tests. Thermostability evaluation was carried out using 1 mL AgNPs samples with a peptide concentration of 20 μ M, and then changes in the absorption spectra were recorded at 0 min, 15 min, 45 min and 2 h of heating at 98°C. Further, AgNP@peptide replaced capped agent (100 μ M peptide final concentration) were centrifuged using a Sorval™ ST16 centrifuge (Thermo Fisher Scientific, Massachusetts, USA) at 1000, 2500 and 3000 rpms, variations were followed measuring the changes in the SPB spectra. Finally, the pH stability of the AgNPs with ensuing changes in pH was done using a 0.1 M stock solution of sodium hydroxide and following the SPB spectral changes.

Preparation type I collagen injectable hydrogel - AgNP@peptide embedded within

Hydrogels were prepared on ice in 1 mL aliquots, using a T-piece system, by mixing a solution of Type I medical grade porcine collagen Theracol at 1% (~10 – 11 mg/ml) with 1xPBS and 40% chondroitin sulphate; EDC/NHS chemistry was then used to encourage the crosslinking of the hydrogel by adding a 1:1 mixture of the two reagents as well as NaOH to the solution. Additionally, 180 μ M solution of AgNP@peptide (p2 or P3) previously freeze-dried and resuspended in MilliQ water was prepared, and then added such that the final mixture contained a concentration was 18 μ M AgNP@peptide. After 10 cycles through the T-piece system, the solution was plated and allowed to cross-link for 30 minutes while incubated at 37°C. Finally, the gels were washed 3 times with 1xPBS and subjected to biocompatibility testing and a stability test was also performed where the SPB was measured after 1 and 7 days.

***In vitro* assessments**

The antibacterial activity of the materials was assessed by incorporating freshly prepared overnight cultures of *Pseudomonas aeruginosa* (PAO1; 1×10^5 cfu/mL) onto the different hydrogels containing the nanoparticles capped with peptides P2 and P3 and then incubated overnight at 37°C. Spectral scanning and plate counting was used to determine the bactericidal effects of the nanomaterial.

Human dermal fibroblasts cell line (ATTC) transfected with green fluorescence protein (GFP) was cultured in DMEM media supplemented with 10% fetal bovine serum (FBS), 1% penicillin, 1% streptomycin and 0.1% gentamicin. Cells were grown at 37°C with 5% CO₂. Media was changed every 2 days and cells were passaged at 90% confluency using 0.5% trypsin EDTA solution. In a 48 well-plate, around 10,000 cells per well were seeded over hydrogels containing the different peptides and then incubating at 37°C. Cell toxicity was evaluated by imaging the cells every 24 h up to 72 h, using a JuLI™ FL fluorescence live cell movie analyser (NanoEntek, Pleasanton, USA).

Generation of Atomistic Models

The molecular structures of all the peptides were constructed and optimized using Chimera² software. The Ag{111} surface was constructed with a lattice parameter of 4.165 Å according to the model of Hughes et al.³ The Hughes supercell surface was replicated two times in *x* and *y* direction giving a surface area of 7 nm². 5.0 and 6.2 nm of water molecules were placed above and below the Ag{111} surface for P1-P2 and P3 respectively, giving equilibrium height of ~4.8 and ~5.8 nm along the *z*-axis, respectively. The simulation box was periodic along all three axes. All the systems were assembled using VMD 1.9.2 software.⁴

Molecular Dynamics Simulations

All simulations were executed in the molecular dynamics software NAMD 2.12⁵, employing the standard TIP3P water model used by the CHARMM force field.^{6, 7} The temperature and pressure were maintained at 300 K and 101.325 kPa (1.0 atm), respectively, by the Langevin thermostat and Langevin piston⁸ methods. The area of the systems was fixed in the xy -plane, and the Langevin piston acted only along the z -axis. A smooth 0.8–0.9 nm cutoff of van der Waals forces was employed. The equation of motion was integrated with a time step of 4 fs, which was permitted by an increase of the masses of nonwater hydrogen atoms in a factor of 3 (to 3.0240 Da), transferring mass from the heavy atom to which they were attached.⁹ For each peptide-AgNP (P1, P2 and P3) system, we performed 20000 steps of energy minimization followed by 10 ns of equilibration before beginning the free energy calculation. VMD 1.9.2 was used for visualization and molecular renderings.⁴

Free Energy Calculations

Using a starting point equilibrated system, the adaptive biasing force¹⁰⁻¹³ method was applied to calculate the free energy as a function of two transition coordinates: $Z = z(\text{peptide}) - z(\text{Ag})$ to sample the distance from the peptide to the Ag surface, and $\zeta = z(\text{res5}) - z(\text{res1})$ to sample the orientation of the free-energy peptide relative to the surface. The adaptive biasing force method was implemented through the Colvars module¹⁴ of NAMD 2.12.⁵ The first collective variable, Z , was sampled using multiple windows (one single window for P1; three windows, 4–16, 15–22 and 20–28 Å, for P2 and P3), and the second collective variable was sampled using a single window $-25 \leq \zeta \leq 25 \text{Å}$ for a total simulated time of 1000 ns, 1917 ns, and 2067 ns for P1, P2 and P3 respectively. This approach was previously used by our group and explained more in detail in Poblete et al.¹⁵

To demonstrate that the thiol acts to anchor the peptide to the surface, that it holds on as long as possible even when the center of mass of the peptide is relatively far from the surface, we calculated the mean distance between the surface and the thiol sulfur atom as a function of the distance between the surface and the center of mass (Z). To do this, we binned frames of the MD trajectory according to the value of the transition coordinate Z in bins of size $\Delta Z = 0.5 \text{Å}$. For each bin b , we calculate the mean position of

the sulfur atom as the weighted average¹⁶

$$\langle z_S(Z_b) \rangle = \frac{\sum_i z_S^i \exp(-\beta w(Z_i, \zeta_i))}{\sum_i \exp(-\beta w(Z_i, \zeta_i))},$$

where the sums run over all frames i for which the transition coordinate Z is in bin b , Z_i and ζ_i are the values of the transition coordinates in frame i , z_S^i is the distance between the surface and the thiol sulfur atom in frame i , $w(Z_i, \zeta_i)$ is the value of the potential of mean force on the two transition coordinates in frame i , and $\beta=1/(k_B T)$ is the inverse thermal energy.

Statistical analyses

Student's t-test (unpaired data with unequal variance) using a confidence interval of $p < 0.05$ was considered to identify statistically significant differences. Analyses were carried out in Kaleida Graph 4.5®.

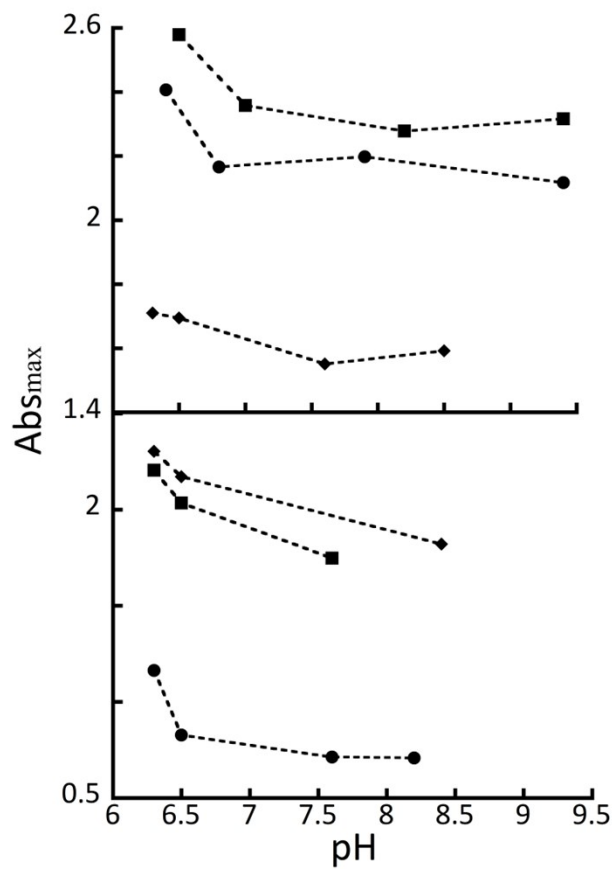


Figure S1. Effect of pH changes on the maximum absorption of AgNPs where the capping agent was replaced with CLK-GP-Hyp (●), CLK-(GP-Hyp)₃ (■), and CLK-(GP-Hyp)₅ (◆) at 20 μM (Top) and 100 μM (Bottom) concentrations. All measurements were carried out at room temperature and by triplicate with different batches.

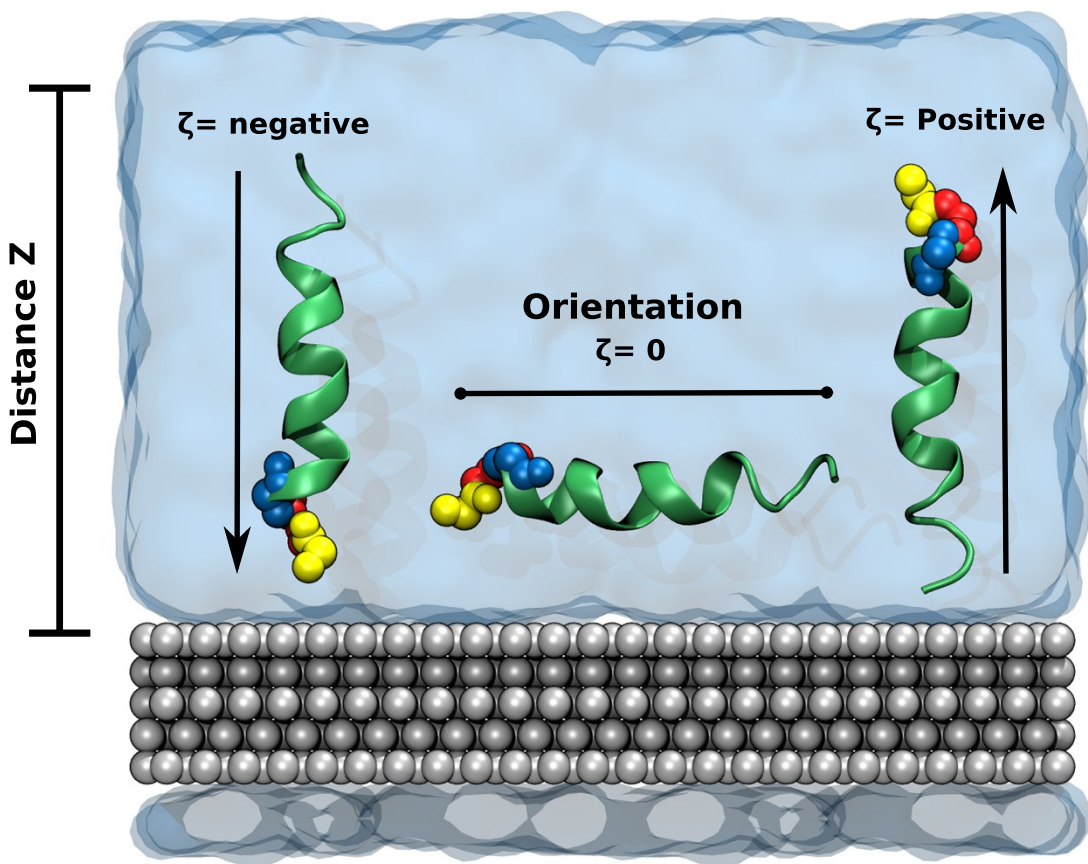


Figure S2. Peptide-AgNP molecular dynamics model. Water is shown as a transparent blue surface while silver atoms are shown as a gray spheres. The peptide is represented as green cartoon structure, and cysteine, leucine and lysine are shown as yellow, red and blue spheres, respectively. Left, diagram of the Z transition coordinate, which is the distance between the center of mass of the peptide and the plane passing through the first layer of silver atoms. Second transition coordinate: Orientation (ζ), which is the difference in the z coordinates between the centers of mass of the last residue and the first residue for each peptide.

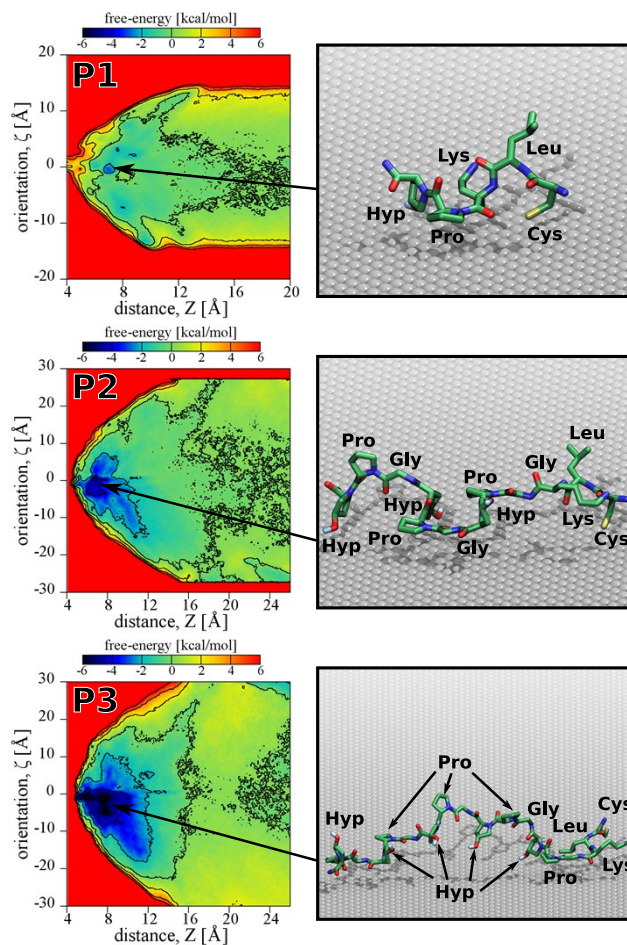


Figure S3. Molecular simulations of the adsorption of CLK-GP-Hyp (P1), CLK-(GP-Hyp)₃ (P2), and CLK-(GP-Hyp)₅ (P3) to the nanosilver surface. (Left) Two-dimensional free energy landscape for the peptides P1, P2 and P3. By convention, the free energy is anchored to average to zero for large separations of the peptide and surface ($Z > 24$ Å). The black curves represent isoenergetic contours separated by 2 kcal/mol. (Right) Typical conformations of each peptide corresponding to the free energy minima in the two-dimensional free-energy plots indicated by the black arrow. The high-affinity areas (blue) represent conformations in which the peptide interacts most strongly with the surface, while the yellow, green and cyan regions indicate lower affinities. Areas shown in red are high free-energy conformations, corresponding to steric clashes between the surface and peptide (small Z values) or unfavorable extension of the peptide (large ζ values).

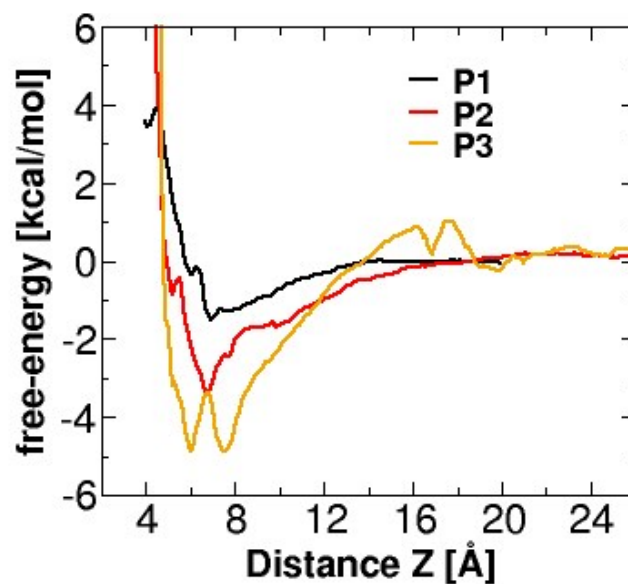


Figure S4. Adsorption free energy of CLK-GP-Hyp (P1), CLK-(GP-Hyp)₃ (P2), and CLK-(GP-Hyp)₅ (P3) on a AgNPs surface. Free energy profiles along the single transition coordinate Z for each peptide. These one-dimensional potentials of mean force were extracted by the integration of the two-dimensional potential of mean force shown in the main text.

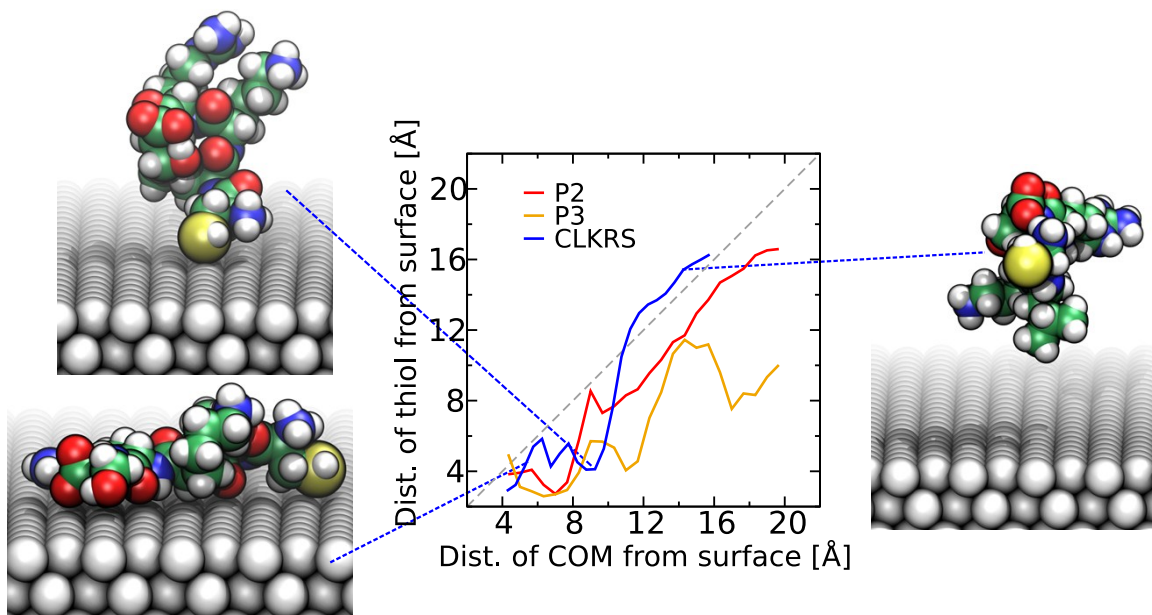


Figure S5. Position of the thiol sulfur atom as a function of the peptide's center of mass position. Plot: Position of the thiol sulfur of the P2, P3 and CLKRS¹⁵ peptides as a function of each peptides center of mass. Pictures: Representative snapshots of the conformations acquired by the peptides as function of the center of mass of the peptide to the surface.

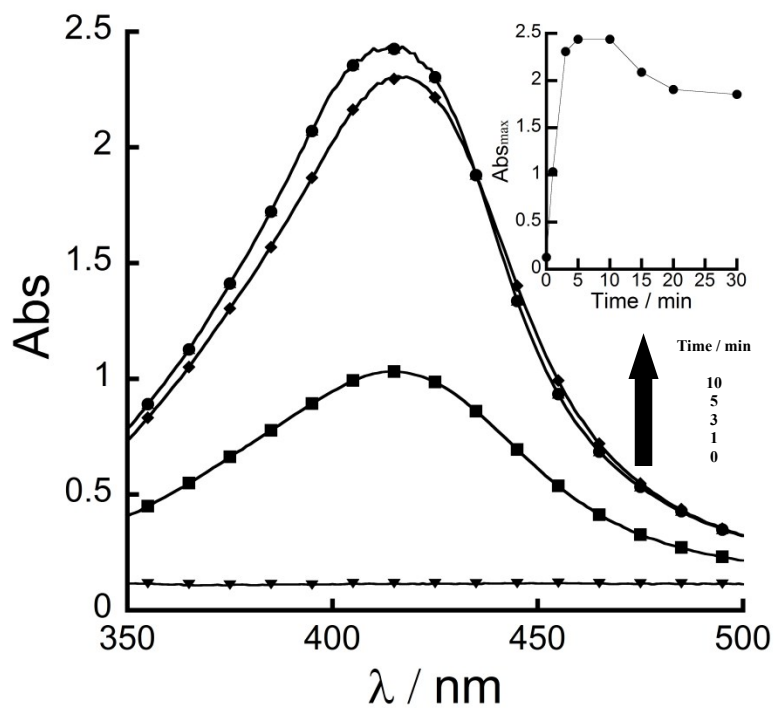


Figure S6. SPB for nanosilver measured at different time points from bottom to top (0, 1, 3 and 5 min) upon UVA irradiation of the solution containing the nanosilver precursors as well as 1 μ M of CLK-(GP-Hyp)₃ (P2). Inset: Representative changes in the SPBs maximal absorption measured at different time intervals during the synthesis. All measurements were carried out at room temperature and by triplicate with different batches.

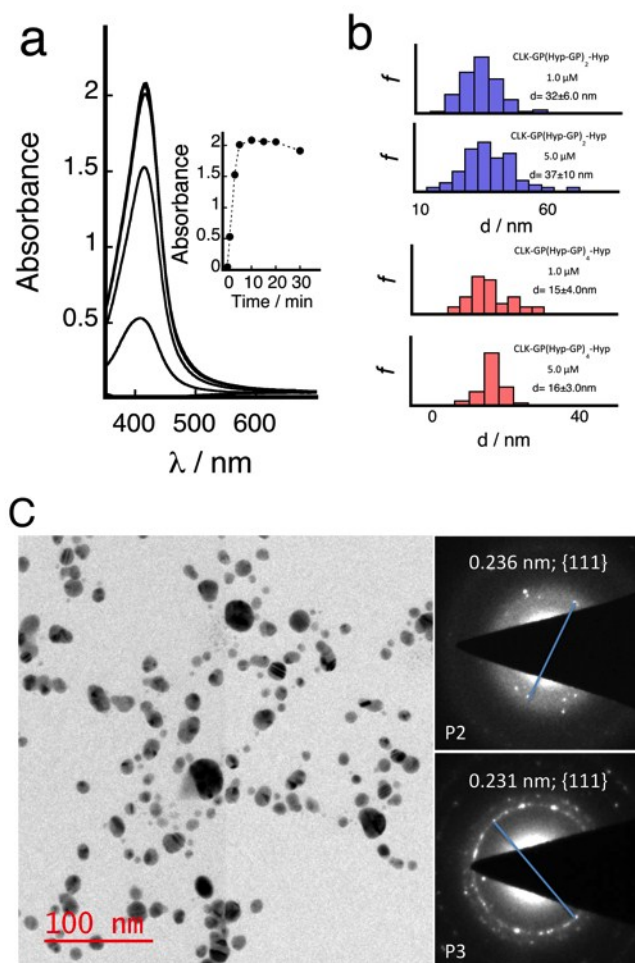


Figure S7. (a) SPB for nanosilver measured at different time points from bottom to top, 0, 1, 3, and 5 minutes upon UVA irradiation of the solution containing the nanosilver precursors in the presence of 1.0 μM of CLK-(GP-Hyp)₅. Inset: Representative changes in the SPB maxima absorption measured at different time intervals during the synthesis. All measurements were carried out at room temperature, see SI for further details. (b) Size histograms for silver nanoparticles prepared using two different concentrations of the peptides CLK-(GP-Hyp)₃ (P2) and CLK-(GP-Hyp)₅ (P3) as protecting agents for photochemically formed nanosilver. Histograms were constructed by measuring 100 individual nanoparticles from TEM images. Mean number and standard deviations for each population are shown in the figures. (c) **Left:** Representative TEM images for silver nanoparticles prepared using 1.0 μM CLK-(GP-Hyp)₅ (P3). **Right:** Diffraction patterns for silver nanoparticles prepared using 1.0 of CLK-(GP-Hyp)₃ (P2, top) or CLK-(GP-Hyp)₅ (P3, bottom).

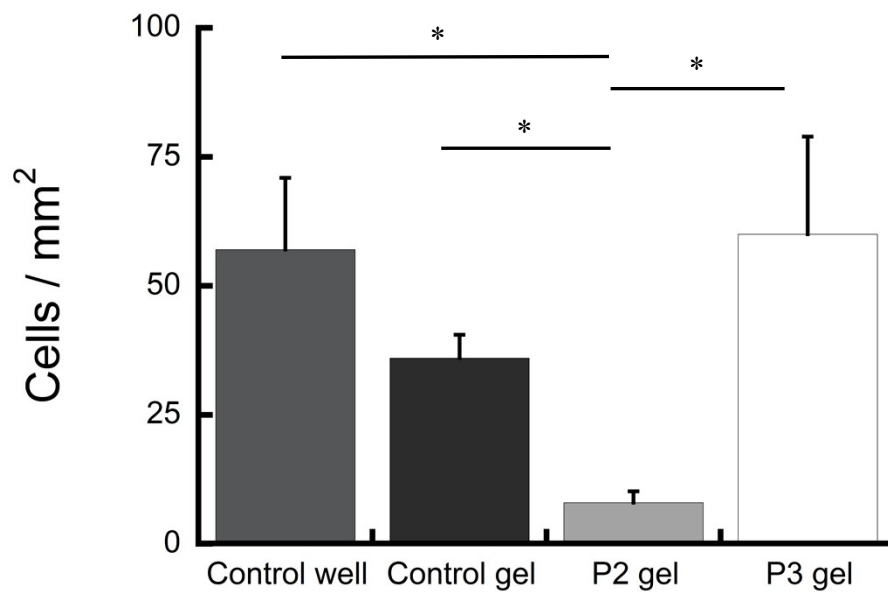


Figure S8. Results from the manual counting of skin fibroblasts after a 24h incubation period at 37°C within either a control well, a well containing a control gel or a well containing a gel imbedded with CLK-(GP-Hyp)₃ (P2) or CLK-(GP-Hyp)₅ (P3) linked to AgNPs. Each category was made in triplicate. *p<0.05

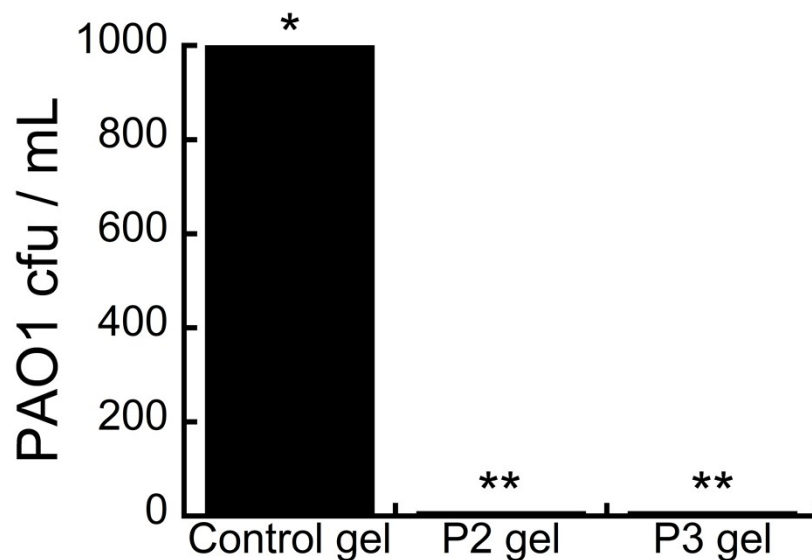


Figure S9. Results from the manual counting of *Pseudomonas aeruginosa* (PAO1 at 10^5 cfu/mL) after overnight incubation within either a control well, a well containing a control gel or a well containing a gel imbedded with CLK-(GP-Hyp)₃ (P2) or CLK-(GP-Hyp)₅ (P3) linked to AgNPs. Each category was made in triplicate and each well had bacterial plates made in duplicate for a total of six bacterial plates made per category. *Bacterial colonies surpassed the counting limit. **None detected in agar plates.

References

1. E. I. Alarcon, K. Udekwi, M. Skog, N. L. Pacioni, K. G. Stamplecoskie, M. Gonzalez-Bejar, N. Polisetti, A. Wickham, A. Richter-Dahlfors, M. Griffith and J. C. Scaiano, *Biomaterials*, 2012, **33**, 4947-4956.
2. E. F. Pettersen, T. D. Goddard, C. C. Huang, G. S. Couch, D. M. Greenblatt, E. C. Meng and T. E. Ferrin, *J Comput Chem*, 2004, **25**, 1605-1612.
3. Z. E. Hughes, L. B. Wright and T. R. Walsh, *Langmuir*, 2013, **29**, 13217-13229.
4. W. Humphrey, A. Dalke and K. Schulten, *J Mol Graph*, 1996, **14**, 33-38, 27-38.
5. J. C. Phillips, R. Braun, W. Wang, J. Gumbart, E. Tajkhorshid, E. Villa, C. Chipot, R. D. Skeel, L. Kale and K. Schulten, *J Comput Chem*, 2005, **26**, 1781-1802.
6. R. B. Best, X. Zhu, J. Shim, P. E. Lopes, J. Mittal, M. Feig and A. D. Mackerell, Jr., *J Chem Theory Comput*, 2012, **8**, 3257-3273.
7. A. D. Mackerell, D. Bashford, M. Bellott, R. L. Dunbrack, J. D. Evanseck, M. J. Field, S. Fischer, J. Gao, H. Guo, S. Ha, D. Joseph-McCarthy, L. Kuchnir, K. Kuczera, F. T. Lau, C. Mattos, S. Michnick, T. Ngo, D. T. Nguyen, B. Prodhom, W. E. Reiher, B. Roux, M. Schlenkrich, J. C. Smith, R. Stote, J. Straub, M. Watanabe, J. Wiorkiewicz-Kuczera, D. Yin and M. Karplus, *J Phys Chem B*, 1998, **102**, 3586-3616.
8. S. E. Feller, Y. H. Zhang, R. W. Pastor and B. R. Brooks, *J Chem Phys*, 1995, **103**, 4613-4621.
9. C. W. Hopkins, S. Le Grand, R. C. Walker and A. E. Roitberg, *Journal of Chemical Theory and Computation*, 2015, **11**, 1864-1874.
10. J. Comer, J. C. Gumbart, J. Henin, T. Lelievre, A. Pohorille and C. Chipot, *J Phys Chem B*, 2015, **119**, 1129-1151.
11. E. Darve and A. Pohorille, *J Chem Phys*, 2001, **115**, 9169-9183.
12. J. Henin and C. Chipot, *J Chem Phys*, 2004, **121**, 2904-2914.
13. J. Comer, J. C. Phillips, K. Schulten and C. Chipot, *J Chem Theory Comput*, 2014, **10**, 5276-5285.
14. G. Fiorin, M. L. Klein and J. Henin, *Mol Phys*, 2013, **111**, 3345-3362.
15. H. Poblete, A. Agarwal, S. S. Thomas, C. Bohne, R. Ravichandran, J. Phospase, J. Comer and E. I. Alarcon, *Langmuir*, 2016, **32**, 265-273.
16. A. M. Ferrenberg and R. H. Swendsen, *Phys. Rev. Lett.*, 1988, **61**, 2635-2638.